SUPPORTING INFORMATION

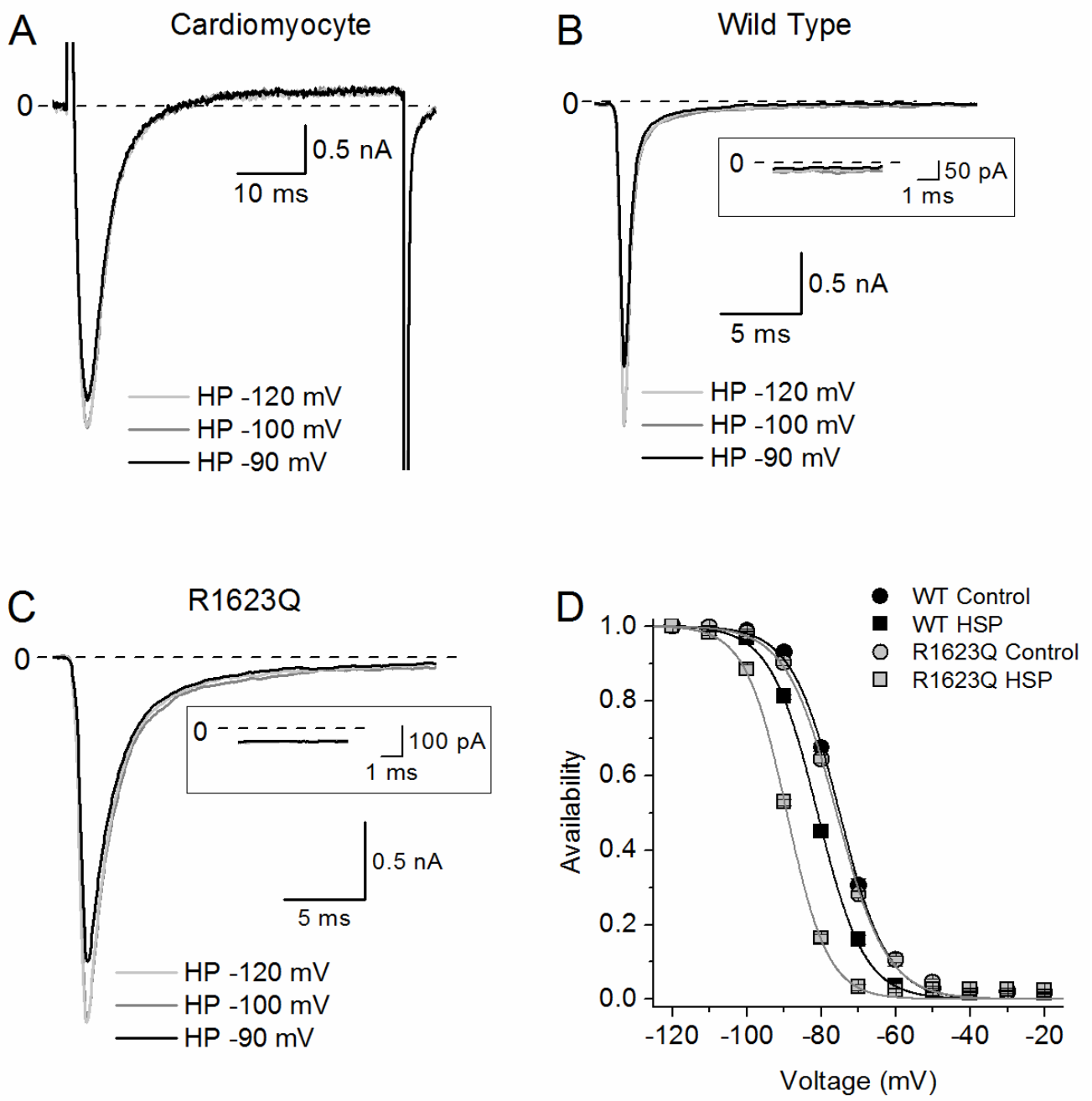

Figure S1. - Peak I_{Na} is saturated at a holding potential of -100 mV.

A.- Representative recordings of I_{Na} in a cardiomyocyte at HP of -120, -100 and -90 mV using a 10 mmol·L^{-1} extracellular Na^+ solution and test pulses to -40 mV. $I_{Na\text{-}Peak}$ was identical at HP of -120 and -100 mV. A small decrease is only seen at HP = -90 mV. $I_{Na\text{-}Peak}$ density was compared in 5 cardiomyocytes at HP of -120 and -100 mV and yielded values of -21.8 ± 1.3 pA·pF^{-1} and -21.9 ± 1.2

pA·pF^{-1}, respectively (not statistically significant; n = 5 cells isolated from 5 hearts; paired t-test). **B.-** Recordings obtained in a HEK293T cell expressing the human WT Na$_V$1.5 channel. I_{Na} was evoked at a test potential of -20 mV. For the sake of clarity only the first 25 ms of the current recordings are shown. The inset shows the last 5 ms (from 45 ms to 50 ms) of the current recording. $I_{Na\text{-}Peak}$ density was compared in 7 cells at HP of -120 and -100 mV and yielded values of -91 ± 12 pA·pF^{-1} and -88 ± 8 pA·pF^{-1}, respectively (not statistically significant; n = 7; paired t-test). **C.-** Recordings obtained in a HEK293T cell expressing the human R1623Q Na$_V$1.5 channel. I_{Na} was evoked at a test potential of -20 mV. For the sake of clarity only the first 25 ms of the current recording are shown. The inset shows the last 5 ms (from 45 ms to 50 ms) of the current recording. $I_{Na\text{-}Peak}$ density was compared in 7 cells at HP of -120 and -100 mV and yielded values of -96 ± 13 pA·pF^{-1} and -90 ± 10 pA·pF^{-1}, respectively (not statistically significant; n = 7; paired t-test). As expected, since $I_{Na\text{-}Peak}$ amplitudes were not significantly different at the HP of -120 and -100 mV, availability curves obtained from HP -120 mV (**D**) were not significantly different to the ones obtained from a HP of -100 mV (see Figure 6C, D). The dots represent the mean ± s.e.m. (n = 13) of the availability curve (in HEK293T cells) for WT and R1623Q in control and in the presence of 100 µmol·L^{-1} HSP. V_{inac} and s_{inac} obtained from a HP of -120 mV were -74.4 ± 0.6 mV and 6.5 ± 0.3 mV and -76.2 ± 0.4 mV and 6.8 ± 0.3 mV in the WT and the R1623Q mutant channel, respectively (not significantly different to the ones obtained from a HP of -100 mV). HSP significantly shifted the availability curve compared to control in both the WT and R1623Q channels. V_{inac} and s_{inac} were -80.8 ± 0.8 mV and 6.3 ± 0.2 mV and -88.3 ± 0.6 mV and 5.5 ± 0.3 mV in the WT and the R1623Q mutant channel, respectively ($P < 0.05$; paired t-test). The shifts induced by HSP on the WT and R1623Q availability curves were not significantly different to the ones obtained from a HP of -100 mV (see Figure 6C, D).

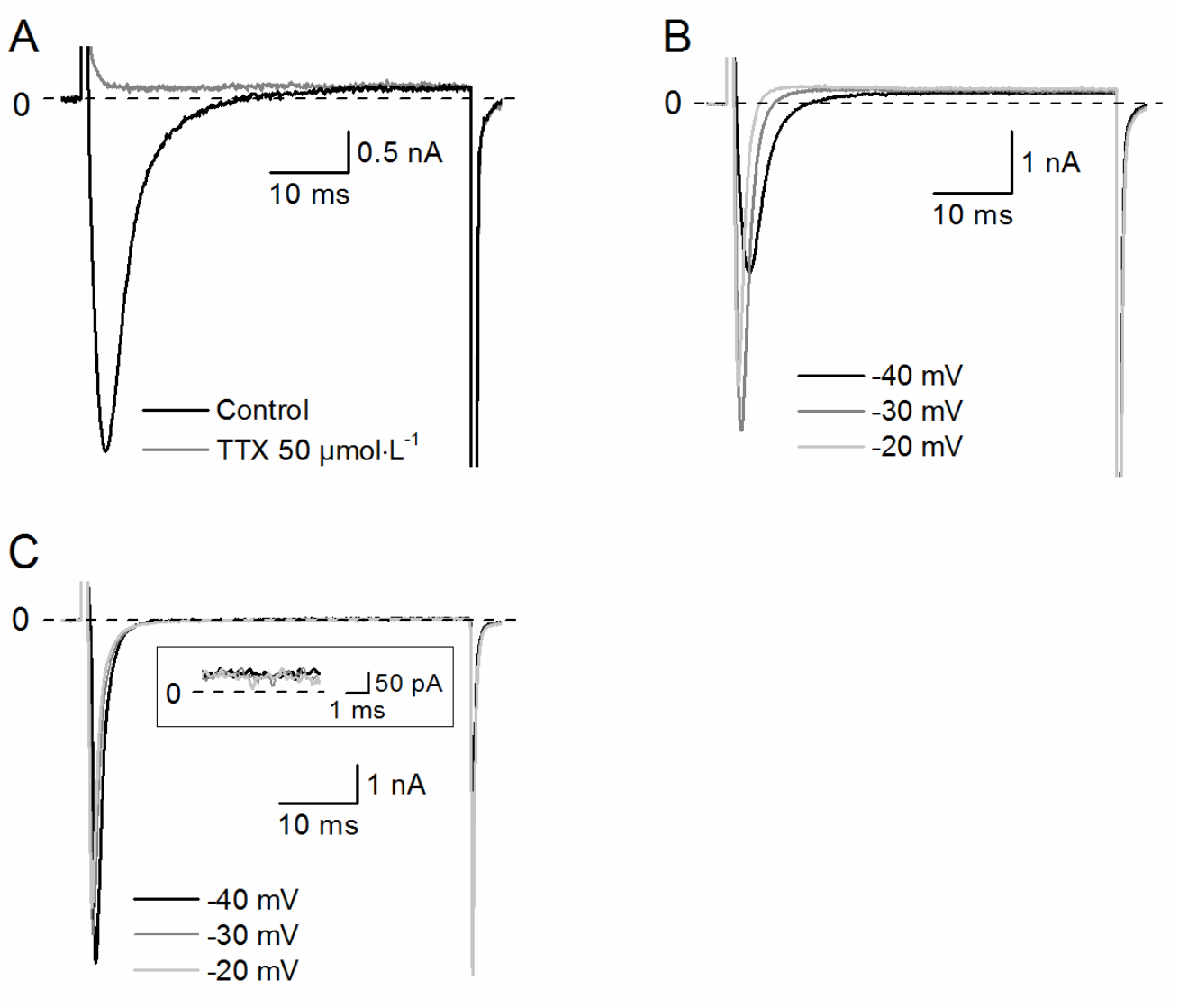

Figure S2. - Absence of $I_{Na\text{-}Late}$ in rat ventricular cardiomyocytes.

A.- I_{Na} recorded at -40 mV in a cardiomyocyte clamped at a HP of -100 mV; extracellular Na^+ concentration was 10 mmol·L^{-1}. Recordings were obtained under control condition and in the presence of tetrodotoxin (TTX, 50 µmol·L^{-1}; n = 5). Note that I_{Na} was completely blocked by TTX and that the current level at the end of the voltage-clamp pulse was the same in both conditions. This indicates that there was no late steady-state inward current at the end of the pulse in control condition. **B.-** I_{Na} recorded at different test potentials from a HP of -100 mV. Extracellular Na^+ was 10 mmol·L^{-1}. Note that not only at -40 mV but also at more depolarized test potentials (-30 and -20 mV), no $I_{Na\text{-}Late}$ was observed (n = 5). Instead, a small steady outward current was more evident at these potentials. **C.-** In

order to rule out any influence of the low extracellular Na^+ concentration on the presence or not of $I_{Na-Late}$, we performed I_{Na} recordings in rat ventricular cardiomyocytes at 117 $mmol \cdot L^{-1}$ extracellular Na^+ concentration. Although there was no voltage control under this condition, no $I_{Na-Late}$ could be recorded at test potentials between -40 and -20 mV (n = 5). The inset shows the last 5 ms (from 45 ms to 50 ms) of the current recording. In cardiomyocytes, the steady outward current at the end of the voltage-clamp pulse is related to the electrogenic Na^+-Ca^{2+}X current, which at the Na^+ and Ca^{2+} concentrations used for cardiomyocytes has a reversal potential around -60 mV. Therefore, at more depolarized potentials the Na^+-Ca^{2+} exchanger exhibits a small outward current.

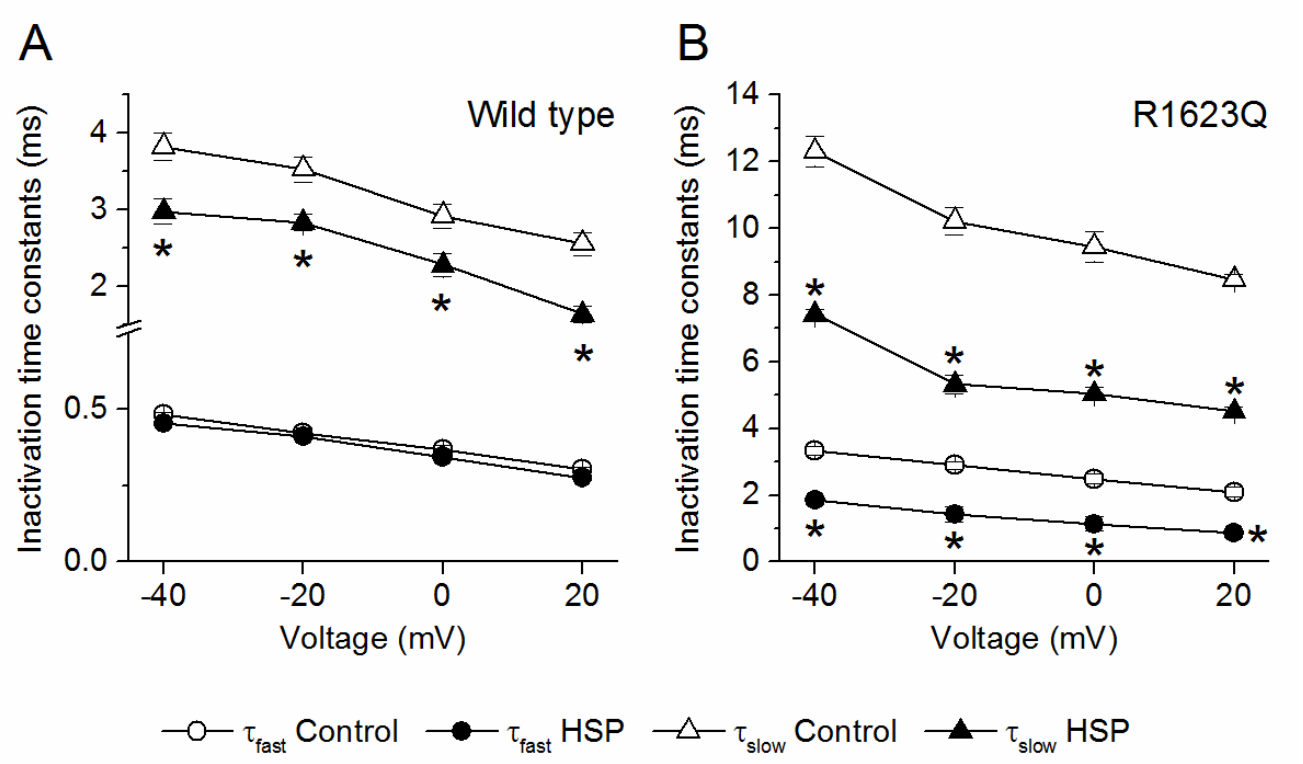

Figure S3. - Voltage dependency of inactivation time constants of I_{Na}.

Inactivation time constants τ_{fast} and τ_{slow} in control conditions and in the presence of HSP (100 µmol·L^{-1}) in HEK293T cells expressing WT (**A**) and R1623Q (**B**) channels. HSP significantly decreased τ_{fast} only in the R1623Q mutant but significantly decreased τ_{slow} in both WT and mutant channels although the decrease in τ_{slow} was more marked in the mutant. * $P < 0.05$ with respect to control; n = 12; one-way ANOVA with Tukey's post hoc test. Note that the effects of HSP on inactivation time constants were not voltage-dependent and the reduction by HSP was proportional at all voltages studied.

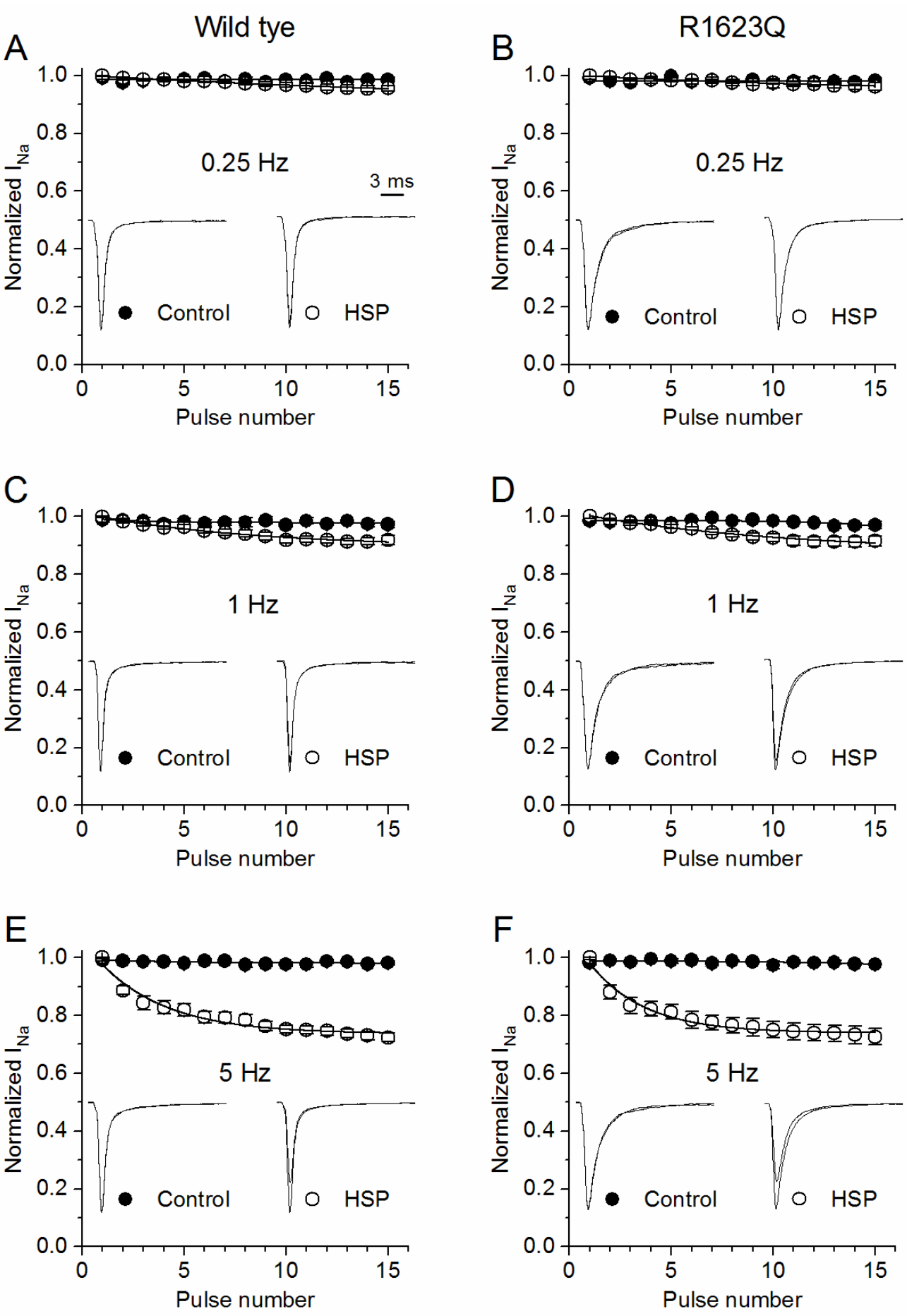
A
Wild tye
B
R1623Q
C
D
E
F
0.25 Hz
1 Hz
5 Hz
3 ms
Control
HSP
Normalized I_{Na}
Pulse number
0.0
0.2
0.4
0.6
0.8
1.0
0
5
10
15

Figure S4. - Tonic and use-dependent block of hesperetin on I_{Na} in WT and R1623Q mutant hNa$_V$1.5 channels.

A to **F.-** Normalized peak I_{Na} at different frequencies of stimulation. The cells were clamped at -100 mV and test pulses to -20 mV were applied at the control frequency (0.25 Hz). Then, stimulation was stopped for 1 min and HSP (100 $\mu mol \cdot L^{-1}$) was perfused during and after this rest period. Subsequently, stimulation was resumed (still in the presence of HSP) at the frequencies shown (A and B: 0.25 Hz; C and D: 1 Hz; E and F: 5 Hz). A first pulse (tonic) block of I_{Na} by HSP (not shown) occurred when stimulation was resumed and was followed by a clear but small use-dependent block at 1 Hz. The tonic block amounted to 94.8 ± 1.8 % and 95.9 ± 1.6 % of total block for WT and R1623Q, respectively, at the lowest frequency (0.25 Hz panels A and B). At 1 Hz the tonic block was 93.3 ± 0.8 % and 90.7 ± 2.7 % of total block for WT and R1623Q, respectively, due to the small use-dependent block (6.8 ± 0.7 % for WT and 9.8 ± 2.9 % for R1623Q; panels C and D). However, at 5 Hz a use-dependent block of HSP on WT and R1623Q hNa$_V$1.5 channels becomes more evident. At this frequency, the tonic block of I_{Na} by HSP was reduced to 72.4 ± 5.3 % and 72.7 ± 5.1 % of total block for WT and R1623Q, respectively, while use-dependent block amounted to 27.7 ± 1.5 % and 27.4 ± 2.9 % of total block for WT and R1623Q, respectively (panels E and F). I_{Na} was normalized by dividing peak current at each pulse by the peak current amplitude at the first pulse after resuming stimulation. The dots represent the mean ± s.e.m. of 6 different cells in each condition. The insets show the corresponding current traces at the 1st and 15th voltage-clamp pulse for both control (black dots) and in the presence of HSP 100 $\mu mol \cdot L^{-1}$; for clarity, only the first 15 ms of the current traces are shown. The 3-ms scale bar shown in panel A is scalable to all current traces in all panels.

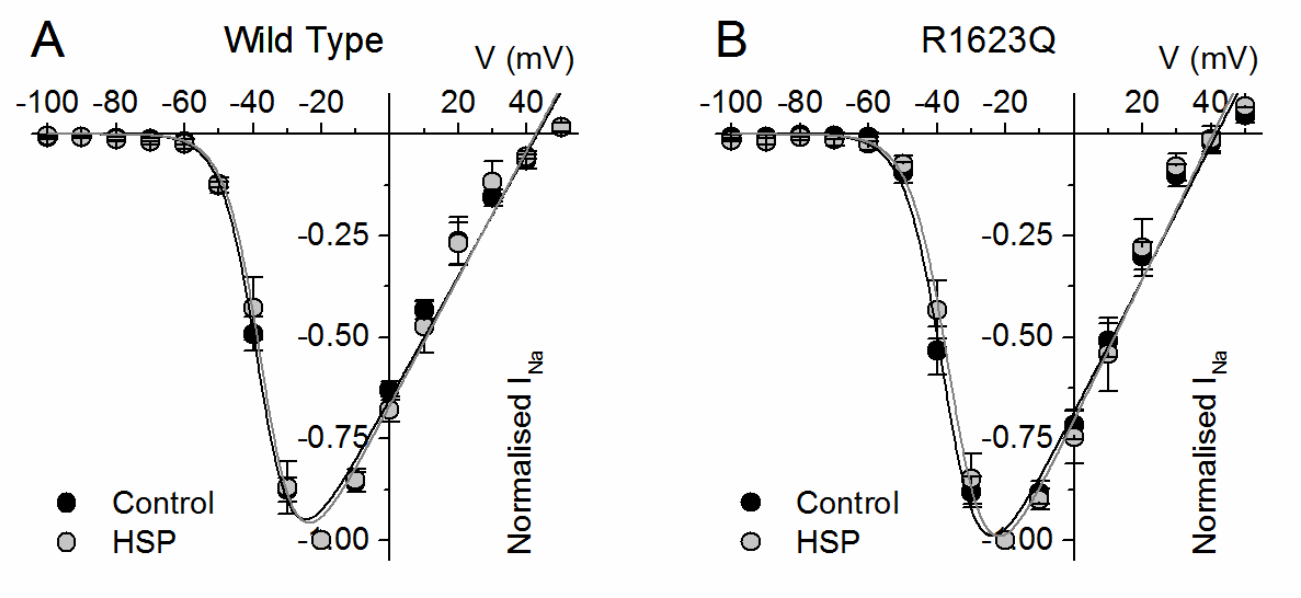

Figure S5. – HSP does not affect the voltage-dependence of channel activation.

Normalised current-to-voltage relationships of I_{Na} in WT (**A**) and R1623Q (**B**) under control condition (black) and in the presence of HSP 100 µmol·L^{-1} (grey). The dots represent the mean ± s.e.m. (n = 13). The similar shape in both curves suggests that HSP does not affect the voltage-dependence of channel activation.

Table 1: Summary table comparing the inhibition potency of hesperetin on the different experimental models studied.

Experimental model	IC_{50} (µmol·L^{-1})	Hill number	Inhibition at maximal concentration tested (%)
Aortic rings (pre-contracted by KCl)	21 ± 11	0.8 ± 0.2	78 ± 13
Aortic rings (pre-contracted by PE)	26 ± 16	0.8 ± 0.4	45 ± 9
Cardiomyocytes I_{Na}	100 ± 14	0.9 ± 0.1	95 ± 3
hNa$_V$1.5 WT $I_{Na\text{-}Peak}$	130 ± 10	0.8 ± 0.1	87 ± 1
hNa$_V$1.5 WT $I_{Na\text{-}10ms}$	54 ± 9	0.6 ± 0.1	89 ± 3
hNa$_V$1.5 WT $I_{Na\text{-}50ms}$	49 ± 5	0.5 ± 0.1	85 ± 1
hNa$_V$1.5 WT $I_{Na\text{-}500ms}$	56 ± 9	0.6 ± 0.1	86 ± 2
hNa$_V$1.5 R1623Q $I_{Na\text{-}Peak}$	136 ± 17	0.8 ± 0.1	90 ± 3
hNa$_V$1.5 R1623Q $I_{Na\text{-}10ms}$	35 ± 4	0.6 ± 0.1	95 ± 2
hNa$_V$1.5 R1623Q $I_{Na\text{-}50ms}$	31 ± 4	0.5 ± 0.1	88 ± 1
hNa$_V$1.5 R1623Q $I_{Na\text{-}500ms}$	32 ± 4	0.6 ± 0.1	93 ± 1
hNa$_V$1.5 F1760A $I_{Na\text{-}Peak}$	N. D.	N. D.	19 ± 2

(N. D.) Not determined. The accuracy of this IC_{50} estimation is compromised due to the very small maximal inhibition.

Table 2: Summary table comparing the values of the parameters obtained from the modified Boltzmann fit of the I-V relationships on the different experimental models studied.

Experimental model	V_{act} (mV)	s_{act} (mV)	V_{inac} (mV)	s_{inac} (mV)
Cardiomyocytes I_{Na} (Control)	-37.1 ± 0.6	4.4 ± 0.5	-71.1 ± 0.2	7.3 ± 0.2
Cardiomyocytes I_{Na} (HSP 100 µmol·L^{-1})	-36.4 ± 0.5	4.9 ± 0.2	-75.1 ± 0.1*	6.9 ± 0.2
hNa$_V$1.5 WT I_{Na} (Control)	-34.7 ± 0.4	4.6 ± 0.3	-74.8 ± 0.3	6.9 ± 0.3
hNa$_V$1.5 WT I_{Na} (HSP 100 µmol·L^{-1})	-34.6 ± 0.4	4.3 ± 0.3	-80.6 ± 0.4*	6.4 ± 0.4
hNa$_V$1.5 R1623Q I_{Na} (Control)	-33.9 ± 0.2	5.5 ± 0.2	-75.4 ± 0.5	7.5 ± 0.4
hNa$_V$1.5 R1623Q I_{Na} (HSP 100 µmol·L^{-1})	-33.5 ± 0.3	5.6 ± 0.2	-87.4 ± 0.8*	5.6 ± 0.7
hNa$_V$1.5 F1760A I_{Na} (Control)	-34.3 ± 0.6	6.4 ± 0.4	-73.2 ± 0.3	6.5 ± 0.3
hNa$_V$1.5 F1760A I_{Na} (HSP 1 mmol·L^{-1})	-35.2 ± 0.4	6.6 ± 0.3	-74.7 ± 0.4	6.8 ± 0.3

* $P < 0.05$ with respect to control condition; paired t-test.

Table 3: Summary table comparing the effects of hesperetin on the I_{Na} activation and availability curves on the different experimental models studied.

Experimental model	V_{act} (mV)	s (mV)	G_{max} (nS·pF^{-1})	V_{Na} (mV)
Cardiomyocytes I_{Na} (Control)	-39.5 ± 0.5	-5.8 ± 0.6	1.2 ± 0.2	-2.2 ± 0.3
Cardiomyocytes I_{Na} (HSP 100 µmol·L^{-1})	-38.0 ± 0.2	-5.2 ± 0.5	0.8 ± 0.1*	-2.9 ± 0.5
hNa$_V$1.5 WT I_{Na} (Control)	-36.7 ± 1.2	-4.5 ± 0.3	1.3 ± 0.1	42.0 ± 0.6
hNa$_V$1.5 WT I_{Na} (HSP 100 µmol·L^{-1})	-33.2 ± 3.3	-4.7 ± 0.7	0.8 ± 0.1*	41.3 ± 0.7
hNa$_V$1.5 R1623Q I_{Na} (Control)	-36.4 ± 1.3	-4.8 ± 0.3	1.5 ± 0.2	40.9 ± 1.3
hNa$_V$1.5 R1623Q I_{Na} (HSP 100 µmol·L^{-1})	-32.4 ± 2.4	-5.4 ± 0.6	1.0 ± 0.1*	38.4 ± 1.7
hNa$_V$1.5 F1760A I_{Na} (Control)	-41.0 ± 1.3	-5.1 ± 0.4	1.8 ± 0.2	42.7 ± 1.1
hNa$_V$1.5 F1760A I_{Na} (HSP 1 mmol·L^{-1})	-39.2 ± 0.7	-4.6 ± 0.4	1.8 ± 0.1	42.2 ± 1.2

* $P < 0.05$ with respect to control condition; paired t-test.

Table 4: Summary table comparing the effects of hesperetin on the time course of the inactivation phase of the I_{Na} traces evoked at -40 mV (cardiomyocytes) or -20 mV (hNa$_V$1.5).

Experimental model	τ_{fast} (ms)	τ_{slow} (ms)	Relative A_{slow} (%)
Cardiomyocytes I_{Na} (Control)	1.30 ± 0.06	9.3 ± 0.3	2.6 ± 0.1
Cardiomyocytes I_{Na} (HSP 100 µmol·L^{-1})	1.27 ± 0.06	8.9 ± 0.3*	2.0 ± 0.1*
hNa$_V$1.5 WT I_{Na} (Control)	0.46 ± 0.02	3.6 ± 0.1	3.2 ± 0.1
hNa$_V$1.5 WT I_{Na} (HSP 100 µmol·L^{-1})	0.41 ± 0.04	2.8 ± 0.1*	2.2 ± 0.1*
hNa$_V$1.5 R1623Q I_{Na} (Control)	2.9 ± 0.1	10.2 ± 0.4	7.2 ± 0.4
hNa$_V$1.5 R1623Q I_{Na} (HSP 100 µmol·L^{-1})	1.4 ± 0.2*	5.3 ± 0.3*	1.9 ± 0.1*
hNa$_V$1.5 F1760A I_{Na} (Control)	0.78 ± 0.02	7.9 ± 0.1	1.3 ± 0.1
hNa$_V$1.5 F1760A I_{Na} (HSP 1 mmol·L^{-1})	0.78 ± 0.01	8.2 ± 0.4	1.4 ± 0.1

* $P < 0.05$ with respect to control condition; paired t-test.